www.elsevier.nl/locate/jorganchem

Journal of Organometallic Chemistry 589 (1999) 191–197

Journal of Organo metallic Chemistry

Syntheses, crystal structures and spectroelectrochemical studies of two isomeric binuclear osmium carbonyl compounds $[\{Os(CO)_2Ph\}_2\{\mu\text{-}\eta^2\text{-}SC(NNPh)_2\}_2]$

Fung-Sze Kong, Wing-Tak Wong *

Department of Chemistry, The University of Hong Kong, Pokfulam Road, Hong Kong, PR China

Received 18 May 1999

Abstract

Treatment of (diphenylthiocarbazono)phenylmercury $[PhHg\{SC(NNPh)_2\}]$ with the triosmium cluster $[Os_3(CO)_{10}(NCMe)_2]$ produced two structural isomers **1a** and **1b** of formulae $[\{Os(CO)_2Ph\}_2\{\mu\text{-}\eta^2\text{-}SC(NNPh)_2\}_2]$ in 35 and 20% yield, respectively. The complexes were fully characterised by IR, ^{1}H-NMR, mass spectroscopies and X-ray crystallography. The isomers **1a** and **1b** show no significant metal–metal interaction and are different in the arrangement of the organic ligand. Complex **1a** was found to undergo a complete conversion to **1b** in the presence of excess reducing agent $Co(Cp)_2$. The electrochemical and spectroelectrochemical (UV–vis) properties of these two complexes are described. © 1999 Elsevier Science S.A. All rights reserved.

Keywords: Osmium; Diphenylthiocarbazono; Spectrochemical

1. Introduction

Dithizone is a well known [1] analytical reagent due to its ability to form intensely coloured, solvent-extractable complexes with a wide variety of metal ions. It is known to undergo both single and double deprotonation reactions. Its best-characterised complexes, however, are those of the monoanion, which is commonly referred to as the 'dithizonate ion', Hdz^- [2]. A number of forms are possible for these complexes given that the dithizonate ion may exist in tautomeric form (Fig. 1). Both tautomers might give rise to linkage isomers. The bidentate N, S chelating form has been established as a 'usual' phenomenon, though unidentate coordination through sulfur has also been characterised recently in indium(III) dithizonate [3], in which two bidentate (N, S) and one monodentate (S) ligands were found. We are interested in exploring the coordination properties of this kind of ligand on a polynuclear metal system. In this context, we have investigated the reaction of mercury complex containing dithizone ligands with

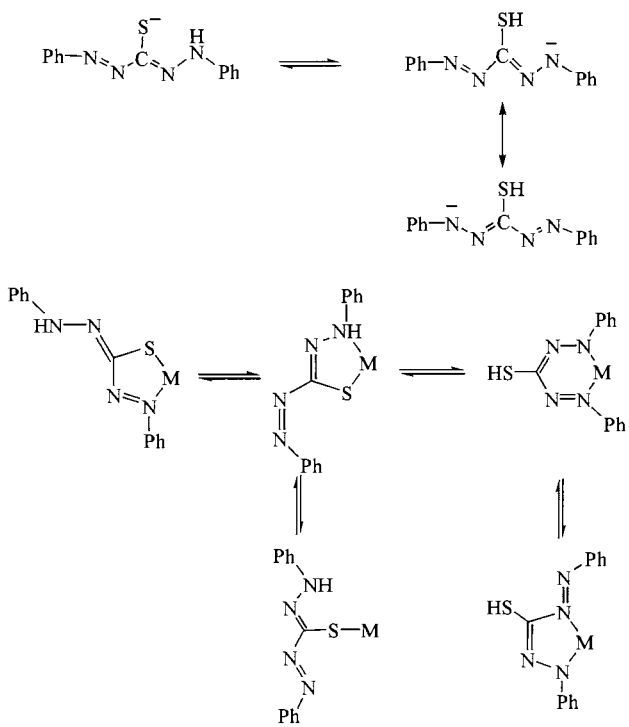

Fig. 1. Isomeric forms of dithizonate ion and its metal complexes.

* Corresponding author. Fax: +852-254-72933.
E-mail address: wtwong@hkucc.hku.hk (W.-T. Wong)

0022-328X/99/$ - see front matter © 1999 Elsevier Science S.A. All rights reserved.
PII: S0022-328X(99)00402-7

Table 1
Spectroscopic data for complexes **1a** and **1b**

Compound	IR ν(CO) (cm^{-1}) [a]	^{1}H-NMR (δ) [b]	FAB MS (m/z) M^+ [c]	λ_{max} [d] (nm) (ϵ 10^{-3} dm^3 mol^{-1} cm^{-1})
1a	2041s, 2020m 1965m, 1954w	8.93 (2H, *s*, NH) 7.38 (4H, *d*, $J = 7.7$, aryl H) 7.30 (4H, *m*, aryl H) 7.04 (22H, *m*, aryl H)	1158 (1158)	232 (43.6) 270 (28.6) 310 (sh) 468 (30.7) 548 (sh) 700 (5.5)
1b	2028vs, 1964s	9.36 (2H, *s*, NH) 7.88 (4H, *m*, aryl H) 7.70 (6H, *m*, aryl H) 7.47 (8H, *m*, aryl H) 7.21 (2H, *m*, aryl H) 6.97 (4H, *m*, aryl H) 6.83 (6H, *m*, aryl H)	1158 (1158)	232 (6.8) 260 (sh) 504 (2.7)

[a] Recorded in CH_2Cl_2; vs, very strong; s, strong; m, medium; w, weak.
[b] Recorded in CD_2Cl_2 at 298 K; s, singlet; m, multiplet.
[c] M^+, parent molecular ion based on ^{192}Os and calculated values in parentheses.
[d] Measured in CH_2Cl_2 at 298 K; sh, shoulder.

triosmium clusters. It has been shown by Au and Wong that oxidation addition of RHgX (R = Me, Et, Ph or Fc; X = Cl, Br or I) to $[Os_3(CO)_{10}(NCMe)_2]$ usually leads to mixed-metal systems of the type $[\{Os_3(CO)_{10}(\mu\text{-}X)\}_2Hg]$ [4]. However, in this report, we describe the isolation of two isomeric binuclear osmium carbonyl complexes containing dithizone ligands instead of mixed-metal clusters using this method. The relationship between this pair of isomers was investigated by UV–vis spectroelectrochemical techniques.

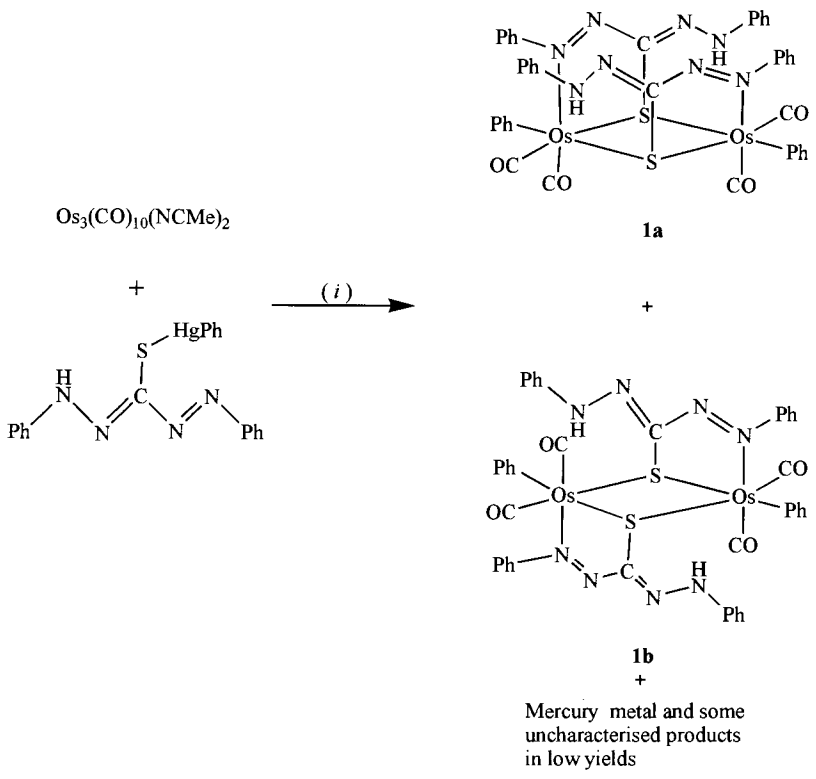

Scheme 1. (i) CH_2Cl_2, r.t.

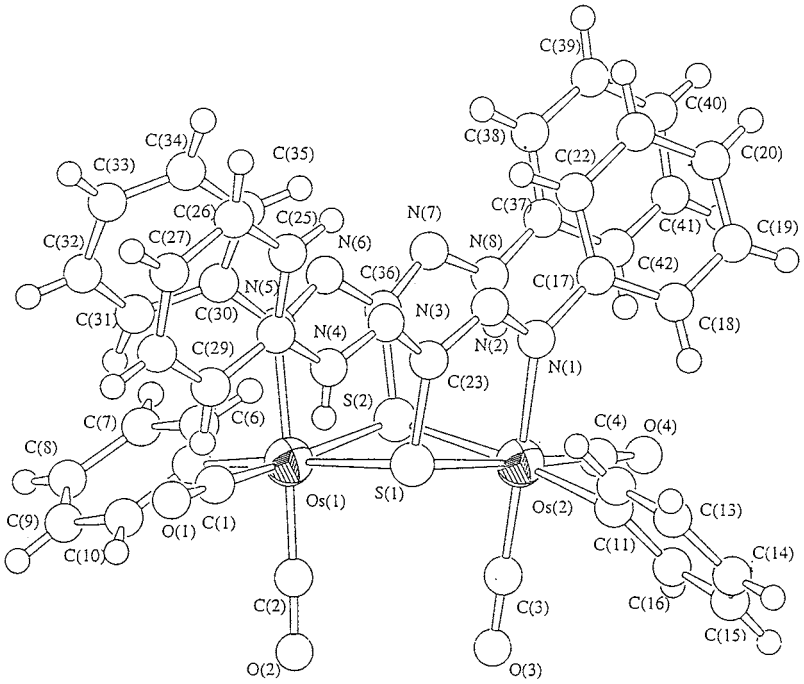

Fig. 2. A perspective drawing of the molecular structure of **1a**.

2. Results and discussion

The reaction of $[Os_3(CO)_{10}(NCMe)_2]$ with $[PhHg\{SC(NNPh)_2\}]$ in dichloromethane at room temperature (r.t.) does not result in any mixed-metal clusters, as expected from the reactions involving organomercurials. This leads to the formation of two binuclear osmium carbonyl isomers of $[\{Os(CO)_2Ph\}_2\text{-}\{\mu\text{-}\eta^2\text{-}SC(NNPh)_2\}_2]$ (**1a**) and (**1b**) in 35 and 20% yields, respectively (Scheme 1). In addition to the mentioned species, metallic mercury and uncharacterised products were obtained. Complexes **1a** and **1b** were isolated in pure form by preparative thin-layer chromatography (TLC) on silica. Only terminal carbonyl activity was observed in the carbonyl absorption region of the IR spectra of **1a** and **1b** in dichloromethane (Table 1). The proton NMR spectra recorded in dichloromethane-d_2 confirm the presence of the organic ligands and the absence of metal hydrides. The mass spectra confirm the isomeric nature of these compounds, where the molecular ion peaks of both compounds appear at $m/z = 1158$ and show a stepwise loss of carbonyls.

Red crystals of **1a** and **1b**, suitable for X-ray analysis, were obtained from benzene–toluene and CH_2Cl_2–*n*-hexane solutions at r.t. Perspective drawings of complexes **1a** and **1b** are shown in Fig. 2 and Fig. 3, respectively, while selected bond lengths and angles are given in Table 2 and Table 3. One molecule of benzene and two molecules of CH_2Cl_2, as the solvent of crystallization, were present in the asymmetric unit of **1a** and **1b**, respectively. X-ray analysis of **1a** and **1b** revealed that the structures consist of two $Os(CO)_2$ fragments, which are held together by two dianions $[\mu\text{-}\eta^2\text{-}SC(NNPh)_2]^{2-}$ bonded through a sulfur and through a nitrogen (N–Os = 2.15 Å). These are in a *syn* and *anti* arrangement with respect to the Os_2S_2 plane for **1a** and

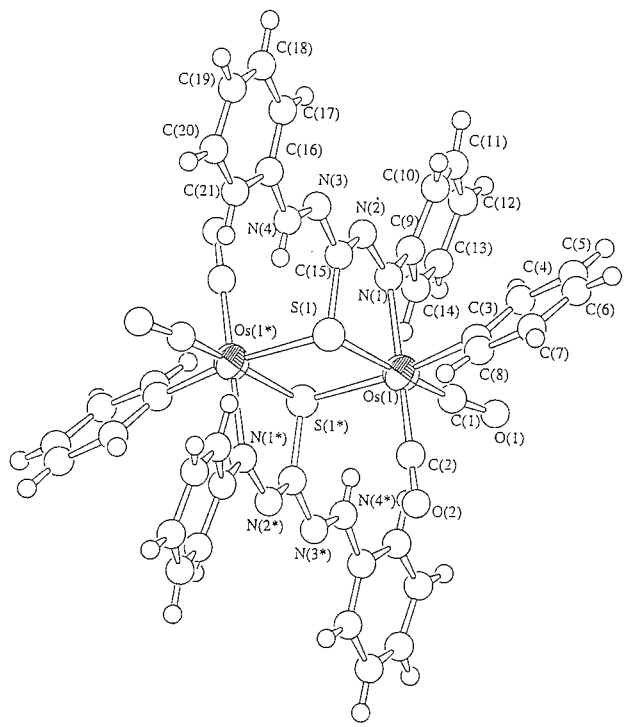

Fig. 3. A perspective drawing of the molecular structure of **1b**.

Table 2
Selected bond length (Å) and bond angles (°) for **1a**

Bond lengths			
Os(1)–S(1)	2.536(4)	Os(2)–S(1)	2.430(4)
Os(1)–S(2)	2.450(4)	Os(2)–S(2)	2.546(4)
Os(1)–N(5)	2.15(1)	Os(2)–N(1)	2.14(1)
Os(1)–C(1)	1.84(2)	Os(1)–C(2)	1.86(2)
Os(1)–C(5)	2.13(2)	Os(2)–C(3)	1.87(2)
Os(2)–C(4)	1.86(2)	Os(2)–C(11)	2.12(2)
S(1)–C(23)	1.77(2)	S(2)–C(36)	1.76(2)
N(1)–N(2)	1.31(2)	N(3)–N(4)	1.31(2)
N(5)–N(6)	1.31(2)	N(7)–N(8)	1.31(2)
N(1)–C(17)	1.45(2)	N(4)–C(24)	1.40(2)
N(5)–C(30)	1.43(2)	N(8)–C(37)	1.38(2)
N(4)–H(37)	0.82(9)	N(8)–H(38)	0.79(9)
Os(1)···Os(2)	3.742(1)	S(1)···S(2)	3.22(1)
Bond angles			
Os(1)–S(1)–Os(2)	97.9(2)	Os(1)–S(2)–Os(2)	97.1(1)
S(1)–Os(1)–S(2)	80.4(1)	S(1)–Os(2)–S(2)	80.6(1)
S(1)–Os(1)–C(1)	92.3(5)	S(1)–Os(1)–C(5)	172.3(4)
S(1)–Os(2)–C(4)	76.6(5)	S(1)–Os(2)–C(11)	93.8(4)
S(2)–Os(1)–C(1)	171.2(5)	S(2)–Os(2)–C(4)	96.1(5)
S(2)–Os(1)–C(5)	92.8(5)	S(2)–Os(2)–C(11)	173.0(4)

1b, respectively. The two sulfur bridges in the Os_2S_2 are asymmetric, Os(1)–S(1) and Os(2)–S(2) being 2.536(4) and 2.450(4) Å, respectively in **1a** and 2.442(9) and 2.544(8) Å in **1b**. The central Os(1)–S(1)–Os(2)–S(2) is not planar in **1a** but adopts an envelope conformation that folds in an angle of 160° with respect to the S(1)···S(2) line. In **1a**, the ligands are essentially planar and *syn*-coordinated to the osmium–sulfur rhombus array (dihedral angles 79.5 and 100.2°) and the molecule possesses C_2 symmetry with a crystallographically imposed two-fold axis passing through the mid-point of the S(1)···S(2) line. By comparing **1b** with the isomer **1a**, the organic ligand is in an *anti*-arrangement, where the molecule contains a centre of inversion which coincides with the crystallographic centre of symmetry. A similar

Table 3
Selected bond length (Å) and bond angles (°) of **1b**

Bond lengths			
Os(1)–S(1)	2.442(9)	Os(2)–S(1 [a])	2.544(8)
Os(1)–C(1)	1.78(5)	Os(1)–C(2)	1.89(3)
Os(1)–C(3)	2.12(3)	Os(1)–N(1)	2.15(2)
S(1)–C(15)	1.73(3)	N(1)–N(2)	1.33(4)
N(3)–N(4)	1.36(3)	N(1)–C(9)	1.43(3)
N(2)–C(15)	1.37(4)	N(3)–C(15)	1.30(4)
N(4)–C(16)	1.41(4)	N(4)–H(16)	0.82(8)
Os(1)···Os(1 [a])	3.741(2)	S(1)···S(1 [a])	3.30(1)
Bond angles			
Os(1)–S(1)–Os(1 [a])	97.3(3)	S(1)–Os(2)–S(1 [a])	82.7(3)
S(1)–Os(1)–C(1)	95(1)	S(1)–Os(2)–C(2)	94.5(1)
S(1)–Os(1)–C(3)	171.0(1)	S(1)–Os(1)–N(1)	79.8(7)
Os(1)–S(1)–C(15)	102.4(9)		

[a] Symmetry code $-x, -y, -z$.

Table 4
Cyclic voltammetry data for [PhHg{SC(NNPh)$_2$}] and complexes **1a** and **1b** [a]

Complexes	Electrochemical processes	
	Oxidation	Reduction
[PhHg{SC(NNPh)$_2$}]	+0.371	−0.843, −1.327
1a	+0.685, +0.382	−1.298, −1.356
1b	+0.656, +0.326	−1.010, −1.250

[a] All potentials measured in V are vs. ferrocene/ferrocenium couple in dry CH_2Cl_2 using a glassy carbon working electrode; 0.1 M [^{n}Bu$_4$N][BF$_4$] as supporting electrolyte; scan rate 100 mV s^{-1}.

ligand disposition has been reported for [$Re_2(CO)_6$(μ-SH){μ-SC(H)PCy$_3$}(NH$_3$)] [5], where the metal is bridged by a carbon instead of a nitrogen atom. The intermetallic distances in both complexes (3.742(1) Å in **1a** and 3.741(1) Å in **1b**) are too long to permit a significant interaction between the two osmium atoms (c.f. average Os–Os distance in [$Os_3(CO)_{12}$] 2.877(3) Å) [6]. A phenyl group is unexpectedly coordinated to the osmium atoms that originated from the cleavage of the Hg–C bond of [PhHg{SC(NNPh)$_2$}]. The Os–C(Ph) bonds in both complexes have a mean distance of 2.13(2) Å, which is similar to that in [(Mes)OsPh{=C(Ph)NHC$_6$H$_4$}] [7] (2.098(6) Å) (Mes = mesitylene).

Around the osmium atoms, the two carbonyl groups are in a facial disposition, where two sulfur atoms and one phenyl group complete a fairly regular octahedral disposition. Since there is no direct metal–metal bond, assuming that two carbonyl groups and one phenyl group donate four electrons and one electron, respectively, the electron count in these pair of isomers requires the dianion to donate five electrons to complete 18 electrons around each metal. As far as the electron count is concerned, both complexes contain 36 cluster valence electrons (CVEs) and are consistent with binuclear complexes that have no metal–metal bond [8].

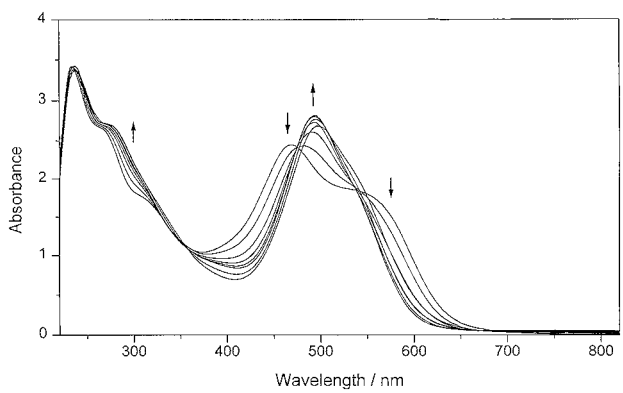

Fig. 4. The UV–vis spectral change accompanying the irreversible oxidation of **1a** producing the isomer **1b** in CH_2Cl_2 at 298 K.

As a consequence of Hg–C and Hg–S bond cleavage, only the [{μ-η^2-SC(NNPh)$_2$}$_2$] moiety is coordinated to the osmium atoms in isomers **1a** and **1b**. The Os(CO)$_2$ unit is derived from the degradation of the parent Os$_3$(CO)$_{10}$ metal core of the starting material, [Os$_3$(CO)$_{10}$(NCMe)$_2$]. A similar, but not strictly comparable example involving the formation of an Os(CO)$_4$ unit, was observed in [Os$_3${μ-AuOs(CO)$_4$(PPh$_3$)}(μ-Cl)(CO)$_{10}$] where the gold atom and the PPh$_3$ ligands are linked in a *trans* configuration through the Os(CO)$_4$ fragment [9]. However, it is tempting to suggest that the [Os$_3$(CO)$_{10}$(NCMe)$_2$] reacted with the mercury reagent in an oxidative addition manner to give some mixed-metal clusters that contain Os–Ph and Os–S linkages. Subsequent cluster degradation led to the formation of **1a** and **1b**. This is consistent with the observation that we have also isolated small amount of metallic mercury and uncharacterised products in the reaction mixture.

The electronic absorption spectral data of isomers **1a** and **1b** are summarised in Table 1. Complex **1a** in CH$_2$Cl$_2$ shows a strong absorption band at 468 and 700 nm with a shoulder at ca. 548 nm. Similarly, the electronic absorption spectrum of complex **1b** in CH$_2$Cl$_2$ shows an absorption band at ca. 504 nm and an absorption tail to longer wavelengths. For the complex [PhHg{SC(NNPh)$_2$}], the spectrum is dominated by three strong absorption bands at ca. 228, 268 and 474 nm, while no significant absorption is observed at wavelengths longer than 500 nm. The bands from ca. 228 to 310 nm correspond to ligand-centred (LC) transitions, while those absorptions in the visible region are likely to be metal-to-ligand or ligand-to-metal charge-transfer transitions (MLCT or LMCT).

The redox properties of isomers **1a** and **1b** were investigated by cyclic voltammetry and UV–vis spectroelectrochemistry. The redox potentials of **1a** and **1b** are presented in Table 4. The cyclic voltammograms show two irreversible reductions and two irreversible oxidation processes for both complexes **1a** and **1b**. The reducing agent, CoCp$_2$, which has a formal reduction potential of 1.94 V (versus ferrocene/ferrocenium), was chosen to react with complex **1a** to afford **1b** as the sole product. The product of this cathodic step was further studied in situ by UV–vis spectroelectrochemistry in a thin-layer cell. Fig. 4 shows the UV–vis spectral changes accompanying the oxidation of **1a** at potential −1.15 V. The UV–vis spectrum shows isosbestic points at 480 and 545 nm, indicating that only two species were present in each oxidation process. The final spectrum is identical to that of **1b**. A similar example observed in the isomerization of *cis*-[ReCl(CO)(dppe)$_2$] into the corresponding *trans* isomer is prompted by oxidation through an electron-transfer chain catalytic process [10]. However, treatment of AgBF$_4$ with **1b** led to insoluble materials instead of **1a**. This suggests that the transformation of **1a** to **1b** was irreversible. There may be interactions between Ag$^+$ salt and the dithizone ligand in **1b** which leads to some other products.

3. Experimental

3.1. Materials and methods

All manipulations were carried out under an inert atmosphere using standard Schlenk techniques, unless stated otherwise. Solvents were purified and distilled from the appropriate drying agents and stored under dinitrogen prior to use. The complex [Os$_3$(CO)$_{10}$-(NCMe)$_2$] was prepared as described previously [11]. (Diphenylthiocarbazono)phenylmercury and bis(cyclopentadienyl)cobalt(II) were obtained from ACROS and STREM Chemicals, respectively. Routine purification of products were carried out in air by thin-layer chromatography (TLC) on plates coated with Merck Kieselgel 60 GF$_{254}$. IR spectra were recorded on a Bio-Rad FTS-7 IR spectrometer using 0.5 mm calcium fluoride solution cells. Proton NMR spectra were recorded in CD$_2$Cl$_2$ on a Bruker DPX 300 FT-NMR spectrometer with SiMe$_4$ as an internal reference. Mass spectra were recorded on a Finnigan MAT 95 spectrometer using fast atom bombardment techniques. Electronic absorption spectra were obtained with a Hewlett–Packard 8452A diode array UV–vis spectrometer. Voltammetric measurements were performed with a Princeton Applied Research (PAR) model 273A potentiostat. The supporting electrolyte was 0.1 M Bu$_4$NBF$_4$ in CH$_2$Cl$_2$. A standard three-electrode cell having a platinum wire counter electrode (Aldrich), an Ag | AgNO$_3$ reference electrode (Bioanalytical) and a glassy carbon working electrode (Bioanalytical) was employed. All measurements were carried out under N$_2$ in anhydrous deoxygenated dichloromethane. A ferrocene/ferrocenium couple was used as an internal reference. Positive-feedback internal resistance compensation was routinely applied.

3.2. Reaction of [Os$_3$(CO)$_{10}$(NCMe)$_2$] with (diphenylthiocarbazono) phenylmercury

A solution of [Os$_3$(CO)$_{10}$(NCMe)$_2$] (100 mg, 0.32 mmol) and [PhHg{SC(NNPh)$_2$}] (28.4 mg, 0.16 mmol) in CH$_2$Cl$_2$ (25 cm^3) was stirred at r.t. until all starting materials had been consumed (2 h, TLC monitoring). The reaction mixture was then filtered to remove the very fine powder of mercury and the filtrate was evaporated in vacuo. Subsequent purification by TLC using CH$_2$Cl$_2$–*n*-hexane (1:1 v/v) as the eluent afforded two consecutive bands, namely isomers **1a** (R_f 0.66; 35 mg, 0.030 mmol, 35%), **1b** (R_f 0.57; 20 mg, 0.017 mmol, 20%) as well as some uncharacterized products (Scheme

Table 5
Crystallographic data for complexes **1a** and **1b**

	1a·C_6H_6	**1b**·$2CH_2Cl_2$
Empirical formula	$C_{48}H_{38}N_8O_4Os_2S_2$	$C_{44}Cl_4H_{36}N_8O_4Os_2S_2$
Formula weight	1235.40	1327.15
Colour	Red	Red
Habit	Block	Block
Crystal size (mm)	$0.22\times0.23\times0.33$	$0.19\times0.22\times0.31$
Crystal system	Triclinic	Triclinic
Space group	$P\bar{1}$ (#2)	$P\bar{1}$ (#2)
a (Å)	14.321(3)	9.792(1)
b (Å)	15.459(3)	10.183(1)
c (Å)	12.099(2)	13.139(2)
α (°)	101.15(2)	77.38(1)
β (°)	102.29(2)	74.99(1)
γ (°)	114.11(2)	76.49(2)
U (Å^3)	2267(1)	1212.9(3)
Z	2	1
D_c (g cm^{-3})	1.809	1.817
F(000)	1196	640
μ(Mo–K$_\alpha$) (cm^{-1})	57.40	55.86
ω Scan width (°)	$(0.79+0.35\tan\theta)$	–
2θ range (°)	45	48.4
Scan speed (deg min^{-1})	16	–
Transmission coefficients	0.7977–1.0000	–
No. reflections collected	5163	8898
No. unique reflections	4877	2082
No. observed reflections [$I>3\sigma(I)$]	2884	1174
R [a]	0.039	0.068
R' [b]	0.043	0.078
g in weighting scheme [c]	0.009	0.023
Goodness-of-fit indicator	1.34	1.39
Maximum Δ/σ	0.05	0.03
No. parameters	277	149
Max, min density in ΔF map (e Å^{-3}), close to Os	0.90, −0.78	1.12, −1.55

[a] $R=\Sigma\|\|F_o|-|F_c\||/|F_o|$.
[b] $R'=[\Sigma\omega(|F_o|-|F_c|)^2/\Sigma\omega F_o^2]^{1/2}$.
[c] $w=[\sigma_c^2(F_o)+g^2/4(F_o^2)]^{-1}$.

1). (Found: C, 49.8; H, 2.8; N, 12.4. Calc. for $C_{42}H_{32}N_8O_4Os_3S_2$ (**1a**): C, 49.7; H, 2.8; N, 12.4%. Found: C, 49.7; H, 2.8; N, 12.5. Calc. for $C_{42}H_{32}N_8O_4Os_3S_2$ (**1b**): C, 49.7; H, 2.8; N, 12.4%.)

3.3. Reaction of complex *1a* with *Co(Cp)$_2$*

A CH_2Cl_2 (20 cm^3) solution of **1a** (50 mg, 0.043 mmol) was stirred with a ten-fold excess of $Co(Cp)_2$ (75.67 mg, 0.40 mmol) at r.t. in a nitrogen atmosphere. The solution turned from reddish–brown to deep purple immediately. The solution was then stirred for a further 2 h when almost all of the starting material was consumed, as checked by TLC. The solvent was then removed and the residue was redissolved in CH_2Cl_2 (2 cm^3). TLC purification (n-hexane–CH_2Cl_2, 50/50 v/v) and IR confirmation indicated that **1b** was isolated as the sole product.

3.4. Reaction of complex *1b* with *AgBF$_4$*

A CH_2Cl_2 solution of excess $AgBF_4$ was added dropwise through a cannular to a CH_2Cl_2 solution of **1b** (50 mg, 0.020 mmol) at r.t. in a nitrogen atmosphere. A purplish solid precipitated immediately. No starting material or **1a** were observed by TLC.

3.5. X-ray data collection and structural determination of complexes *1a* and *1b*

Single crystals of complexes **1a** and **1b** suitable for X-ray analyses were obtained by slow evaporation from a benzene–toluene, and a CH_2Cl_2–n-hexane solution, at r.t. Crystals for all the complexes were mounted in air on a glass fibre with epoxy resin. X-ray diffraction data of complex **1a** was collected at r.t. on a Rigaku AFC7R diffractometer, using graphite-monochromated Mo–K$_\alpha$ radiation ($\lambda=0.71073$ Å) by the ω–2θ scan method. For complex **1b**, data were collected on a MAR research image plate scanner, also with Mo–K$_\alpha$ radiation. A summary of the crystallographic and structure refinement data is listed in Table 5. All intensity data were corrected for Lorentz and polarisation effects. Absorption corrections using the ψ-scan method were also applied for structure **1a**. An approximation to absorption correction by inter-image scaling was made for **1b**. Space groups of the crystals were determined from a Laue symmetry check and their systematic absences and were then confirmed by successful refinement of the structures. The structures were solved by direct methods (SIR92) [12] for **1a** and by the Patterson method (SAPI91) [13] for **1b**, and expanded by Fourier-difference techniques (DIRDIF94) [14]. The solutions were refined by full-matrix least-squares analysis on F. Hydrogen atoms were generated in their ideal positions, except N(H) which was located from a difference Fourier synthesis, and included in the structure factors calculations but not refined. Calculations were performed on a Silicon-Graphics computer, using the program package TEXSAN [15].

4. Supplementary material

Crystallographic data for complexes **1a**, **1b** and **5** (excluding structural factors) have been deposited with the Cambridge Crystallographic Data Centre as supplementary publication numbers CCDC-119655 and

119659, respectively. Copies of this information may be obtained free of charge on application to CCDC, 12 Union Road, Cambridge CB2 1EZ, UK (Fax: +44-1223-336-033; e-mail: deposit@ccdc.cam.ac.uk).

Acknowledgements

We gratefully acknowledge financial support from the Hong Kong Research Grants Council and the University of Hong Kong. F.-S.K. acknowledges the receipt of a postgraduate studentship, administered by the University of Hong Kong.

References

[1] A.I. Vogel, A Textbook of Quantitative Inorganic Analysis, 4th ed., Longman, London, 1978, p. 150, 158.
[2] H.M.H.H. Irving, Dithizone, The Chemical Society, London, 1977.
[3] J. McB. Harrowfield, C. Pakawatchai, A.H. White, J. Chem. Soc. Dalton Trans. (1983) 1109.
[4] Y.K. Au, W.T. Wong, Inorg. Chem. 36 (1997) 2092.
[5] J. Li, D. Miguel, M.D. Morales, V. Riera, Organometallics 17 (1998) 3448.
[6] M.R. Churchill, B.G. DeBoer, Inorg. Chem. 16 (1977) 878.
[7] H. Werner, U. Wecker, K. Peters, H. Georg von Schnering, J. Organomet. Chem. 469 (1994) 205.
[8] D.M.P. Mingos, J. Chem. Soc. Chem. Commun. (1982) 706.
[9] C. Cathey, J. Lewis, P.R. Raithby, M.C. Ramirez de Arellano, J. Chem. Soc. Dalton Trans. (1994) 3331.
[10] M.F.C. Guedes da Silva, C.M.P. Ferreira, J.J.R. Frausto da Silva, A.J.L. Pombeiro, J. Chem. Soc. Dalton Trans. (1998) 4139.
[11] J.N. Nicholls, M.D. Vargas, Inorg. Synth. 28 (1989) 232.
[12] A. Altomare, M.C. Burla, M. Camalli, M. Cascarano, C. Giacovazzo, A. Guagliardi, G. Polidori, SIR92, J. Appl. Crystallogr. 27 (1994) 435.
[13] H.F. Fan, SAPI91: Structure Analysis Programs with Intelligent Control, Rigaku Corporation, Tokyo, Japan.
[14] B.T. Beurskens, G. Admiroal, G. Beurskens, W.P. Bosman, R. de Gelder, R. Isrel, J.M.M. Smits, Technical Report of the Crystallography Laboratory, University of Nijmegen, The Netherlands, 1994.
[15] TEXSAN, Crystal Structure Analysis Package, Molecular Structure Corporation, Houston, TX, 1985 and 1992.